

Sensitivity of *Proteus vulgaris* to Zinc Oxide Nanoparticles (Kesensitifan *Proteus vulgaris* terhadap Nanozarah Zink Oksida)

SINOUVASSANE DJEARAMANE^{1*}, THARANI RAVINTHARAN¹, SHAROLYNNE XIAO TONG LIANG¹, LING SHING WONG²,
MAHADEVA RAO U.S.³ & SENTHILKUMAR BALASUBRAMANIAN⁴

¹Department of Biomedical Science, Faculty of Science, Universiti Tunku Abdul Rahman, 31900 Kampar, Perak Darul Ridzuan, Malaysia

²Life Science Division, Faculty of Health and Life Sciences, INTI International University, 71800 Nilai, Negeri Sembilan Darul Khusus, Malaysia

³Biochemistry Unit, Faculty of Medicine, Universiti Sultan Zainal Abidin, 20400, Kuala Terengganu, Terengganu Darul Iman, Malaysia

⁴Department of Zoology, Thiruvalluvar University, 632115 Vellore, Tamilnadu, India

Received: 25 September 2020/Accepted: 21 September 2021

ABSTRACT

Zinc oxide nanoparticle (ZnO NP) has become a popular choice in nanomedicine and in the treatment of infections. The present study investigated the sensitivity of *Proteus vulgaris* to ZnO NPs. The bacteriostatic and bactericidal effects on *P. vulgaris* were determined by using turbidity and colony count methods. The oxidative stress induced by the treatment of ZnO NPs was evaluated by investigating the level of intracellular reactive oxygen species (ROS) along with lipid peroxidation (LP) analysis. The results showed the highest bacterial growth inhibition of 76.21±1.91 and 87.49±3.29% determined using the turbidity and colony count methods, respectively. The highest oxidative stress effects were observed in *P. vulgaris* exposed to 100 µg/mL of ZnO NPs for 24 h as shown by 510.90±108.53% increase in ROS production and 328.77±44.36% increase in LP level. The Fourier transform infrared spectroscopy (FTIR) spectrum illustrated the possible involvement of functional groups such as amine, alkane, acid and alkene from the bacterial cell wall in allowing the surface attachment of nanoparticles on the bacterial cells. Hence, the present study clearly demonstrated the sensitivity of *P. vulgaris* to ZnO NPs.

Keywords: Antibacterial property; oxidative stress; *Proteus vulgaris*; sensitivity; zinc oxide nanoparticles

ABSTRAK

Nanozarah zink oksida (ZnO NP) telah menjadi pilihan popular dalam nanoperubatan serta dalam rawatan jangkitan. Kajian ini meneliti kesensitifan *Proteus vulgaris* terhadap ZnO NP. Kesan bakteriostatik dan bakterisid *P. vulgaris* ditentukan dengan menggunakan kaedah kekeruhan dan penghitungan koloni. Tekanan oksidatif yang disebabkan oleh rawatan ZnO NP dinilai dengan menentukan tahap spesies oksigen reaktif (ROS) intrasel bersama dengan analisis peroksidasi lipid (LP). Hasil menunjukkan perencatan pertumbuhan bakteria tertinggi iaitu 76.21±1.91 dan 87.49±3.29% masing-masing ditentukan menggunakan kaedah kekeruhan dan penghitungan koloni. Kesan tekanan oksidatif tertinggi diperhatikan pada *P. vulgaris* yang terdedah kepada 100 µg/mL ZnO NP selama 24 jam seperti yang ditunjukkan oleh peningkatan pengeluaran ROS sebanyak 510.90±108.53% dan peningkatan tahap LP sebanyak 328.77±44.36%. Spektrum transformasi Fourier inframerah (FTIR) menunjukkan kemungkinan penglibatan kumpulan berfungsi seperti amina, alkana, asid dan alkena daripada dinding sel bakteria yang membolehkan pelekatan permukaan nanozarah pada sel bakteria. Oleh itu, kajian ini menunjukkan dengan jelas kesensitifan *P. vulgaris* terhadap ZnO NP.

Kata kunci: Kesensitifan; nanozarah zink oksida; *Proteus vulgaris*; sifat antibakteria; tekanan oksidatif

INTRODUCTION

Metal nanoparticles (MNPs) are one of the most studied nanomaterials in biomedical research as the transporter

of therapeutic substances (Kumar & Anthony 2016). Zinc oxide nanoparticle (ZnO NP) is a popular choice for therapeutic applications due to its effective antibacterial

and anticancer properties (Djearmane et al. 2019; Elshama et al. 2018). Although there are many other MNPs like titanium dioxide (TiO₂), silver (Ag) and copper (II) oxide (CuO) currently available in the industry with reported antibacterial, antifungal and anticancer properties, ZnO NP is preferred due to its low toxicity level, higher sensitivity and cheaper cost (Mishra et al. 2017).

ZnO NPs are reported to be the least toxic to human cells as these particles do not cause any disruption to human deoxyribonucleic acid (DNA) but are harmful to bacterial cells (Sirelkhatim et al. 2015). The non-toxic property of ZnO NP is one of the key reasons for its extensive usage in biomedicine as well as in commercial products like skin care products. ZnO NP is also claimed to be compatible to human skin, hence it is accepted to be used in skin care products, clothes and materials that can come in touch with human skin (Mirzaei & Darroudi 2017). In biomedicine, ZnO NP is widely used in treating cancer and inflammation, and is also a suitable agent for healing wounds (Mishra et al. 2017).

In the present study, the sensitivity of Gram-negative bacterium *P. vulgaris* to ZnO NPs was studied through investigating the growth inhibition and oxidative stress effects of ZnO NP on *P. vulgaris*.

MATERIALS AND METHODS

SEM-EDX OF ZINC OXIDE NANOPARTICLES

The ZnO nanopowder (particle size < 100 nm) was purchased from Sigma-Aldrich. The shape and size of the particle were studied by scanning electron microscope (SEM) while the composition of nanopowder was confirmed by energy dispersive X-ray (EDX) using SEM-EDX analyser (6701F -JSM, JOEL, Japan).

TREATMENT OF BACTERIAL CULTURE WITH NPs

Several colonies of *P. vulgaris* from the pure culture were inoculated into 50 mL tube containing nutrient broth (NB). Then, the tube containing the bacterial suspension was incubated using a shaking incubator maintained at 37 °C. The bacterial suspension at 5 h of subculture (mid-exponential phase), with OD of 0.05 at 600 nm, was exposed to 10, 50, and 100 µg/mL of ZnO NPs. A negative control was prepared with bacterial suspension without addition of ZnO NPs and a positive control was prepared by adding 10 µg/mL tetracycline in bacterial suspension. All the tests and controls were prepared in triplicates and incubated for 24 h at 37 °C in a shaking incubator.

GROWTH INHIBITORY TEST TURBIDITY METHOD

The bacterial suspension treated with ZnO NPs and controls were measured at 24 h for the turbidity by UV-VIS spectrophotometer (Biochrom, Libra S4, UK) at OD₆₀₀. In order to avoid the interference of ZnO NPs, OD₆₀₀ of NB with each concentration of ZnO NPs was determined and subtracted from the test reading. The percentage of inhibition on bacterial growth by the effects of ZnO NPs was calculated using (1) (Liang et al. 2020).

$$\text{Percentage of inhibition in bacterial growth} = \frac{\text{OD}_{600} \text{ in negative control} - \text{OD}_{600} \text{ in treatment}}{\text{OD}_{600} \text{ in negative control}} \times 100 \quad (1)$$

COLONY COUNT METHOD

The bacterial suspension treated with ZnO NPs was streaked on Luria Bertani (LB) agar after 24 h treatment along with the negative control which contained bacterial suspension only and the positive control which contained bacterial suspension treated with 10 µg/mL tetracycline using streak plate method. The colonies were counted after being incubated at 37 °C for 24 h. The percentage of decrease in number of bacterial colonies was calculated using (2).

$$\text{Bacterial growth inhibition (\%)} = \frac{\text{No. of colony in negative control} - \text{No. of colony in treatment}}{\text{No. of colony in negative control}} \times 100 \quad (2)$$

DETERMINATION OF ROS AND LP ESTIMATION OF INTRACELLULAR ROS LEVEL

Dichloro-dihydro-fluorescein diacetate (DCFH-DA) is a non-fluorescent and cell-permeable probe that gives high fluorescent when undergoing oxidation in the presence of esterase or reactive oxygen species (ROS) (Reiniers et al. 2017). The ZnO NP-treated bacterial suspensions incubated at 37 °C after 24 h were washed twice to remove the unbound NPs using 1X phosphate buffered saline (PBS) by centrifuging at 6,000 × g for 10 min. Then, the bacterial suspension was incubated with DCFH-DA (0.1 mM) in the dark at 37 °C for 30 min. After incubation, the unreacted dye was removed from the reaction by washing with 1X PBS at 6,000 × g for 10 min. About 100 µL of DCFH-DA-treated samples were transferred to a 96-well plate and the fluorescence intensity was measured using the microtiter plate reader

(BMG labtech, FLUOstar Omega, Germany) at 490/520 nm as the excitation/emission filter (Djearmane et al. 2020; Liang et al. 2020). A positive control was prepared by treating bacterial suspension with 5% hydrogen peroxide (H₂O₂) for 20 min. The percentage of increase in intracellular ROS was calculated by comparing with the negative control that did not contain ZnO NPs using (3).

$$\text{Percentage of increase in intracellular ROS} = \frac{\text{ROS in treatment} - \text{ROS in control}}{\text{ROS in control}} \times 100 \quad (3)$$

MEASUREMENT OF LIPID PEROXIDATION

BODIPY is a fluorophore that is lipid specific. It detects lipid peroxidation on living cells and forms fluorescence that can be detected at wavelength 490/520 nm (Drummen et al. 2002). The ZnO NP- treated bacterial suspensions after incubation at 37 °C for 24 h were washed twice to remove the unbound NPs using 1X PBS by centrifuging at 6,000 × g for 10 min. After each wash, the supernatant was discarded. Then, the bacterial suspension was incubated with BODIPY (0.2 mM) in the dark at 37 °C for 30 min. After incubation, the unreacted dye was removed from the reaction by washing with 1X PBS and centrifuging at 6,000 g for 10 min. The supernatant was discarded, the pellet was then resuspended with 100 µL of 1X PBS and transferred to a 96-well plate to measure the fluorescence intensity using the microtiter plate reader (BMG labtech, FLUOstar Omega, Germany) at 490/520 nm as the excitation/emission filter (Drummen et al. 2002). The positive control contained the bacterial suspension treated with 5% H₂O₂ for 20 min. The percentage of increase in lipid peroxidation (LP) was estimated with respect to the negative control that was devoid of NPs using (4).

$$\text{Percentage increase in LP} = \frac{\text{LP in treatment} - \text{LP in control}}{\text{LP in control}} \times 100 \quad (4)$$

BINDING OF NPS ON BACTERIAL SURFACE

The Fourier transform infrared spectroscopy (FTIR) spectrum was used to identify the functional groups which were responsible for surface attachment of ZnO

NPs on the bacterial cell wall. Dried bacterial sample was ground with potassium bromide (KBr) salts to make homogenised soft powder. The homogenised sample was then added into a sterile mould cast and secured onto a manual hydraulic press at 4000 psi to form a KBr pellet. The FTIR (Perkin-Elmer, Spectrum RX1, United States of America, USA) was used to analyse the KBr pellet and generate the FTIR spectrum from 4000 to 400 cm⁻¹ (Liang et al. 2020).

ANALYSIS FOR STATISTICAL SIGNIFICANCE

All assays were carried out in triplicates and the results are shown in mean ± standard deviation. SPSS version 16 was used to perform one-way analysis of variance (ANOVA) for analysing the statistical significance on the variances induced by ZnO NPs. The significant difference was accepted at $p < 0.05$.

RESULTS AND DISCUSSION

SEM-EDX OF NANO-ZINC OXIDE PARTICLES

The shape, size, and morphology of ZnO NPs powder observed under SEM were as shown in Figure 1(A). With the aid of SEM, ZnO NPs appeared in clusters and circular in shape with mixtures of rods. The size of the ZnO NPs ranged between 46.7 and 56.4 nm, with an average size of 51.8 nm. Similar shape, size, and morphology of ZnO NPs were reported by Liang et al. (2020). EDX analysis (Figure 1(B)) demonstrated the presence of zinc along with oxygen in the nanopowder studied. The carbon appeared in the EDX spectrum may be due to the use of carbon tape for SEM-EDX sample preparation (Varadavenkatesan et al. 2019).

GROWTH PATTERN OF BACTERIA

The growth curve of *P. vulgaris* was as shown in Figure 2. Based on the growth curve, the exponential phase of *P. vulgaris* started at 2 h and lasted until 8 h and the mid-exponential phase was identified at 5 h. The growth of *P. vulgaris* declined from 24 to 48 h. An earlier study by Ranjbar-Omid et al. (2015) reported the existence of the exponential phase until 10 h and the decline phase from 12 to 18 h on *P. mirabilis* grown in Muller- Hinton broth.

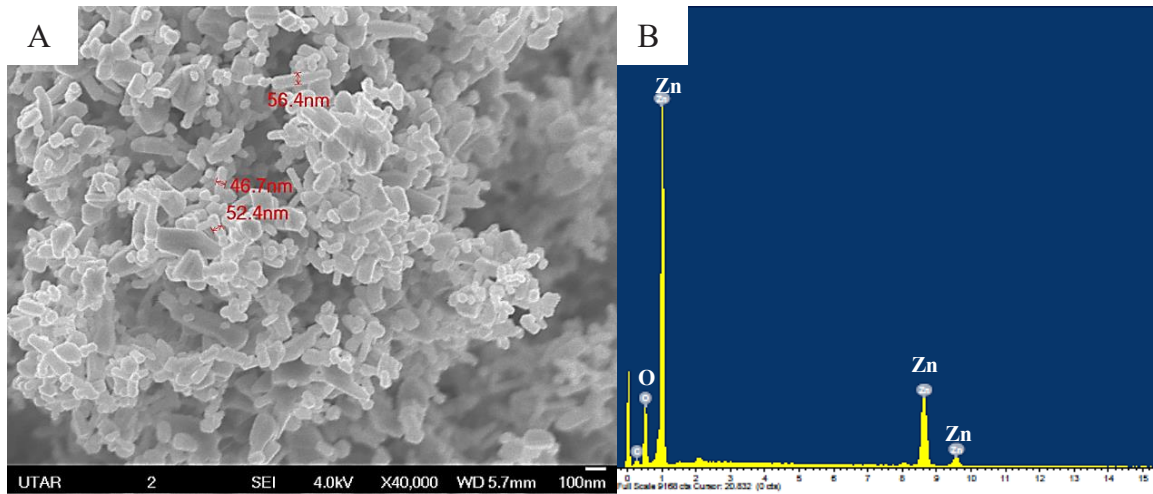


FIGURE 1. Scanning Electron Microscope image (A) and Energy Dispersive X-ray analysis (B) of zinc oxide nanopowder.

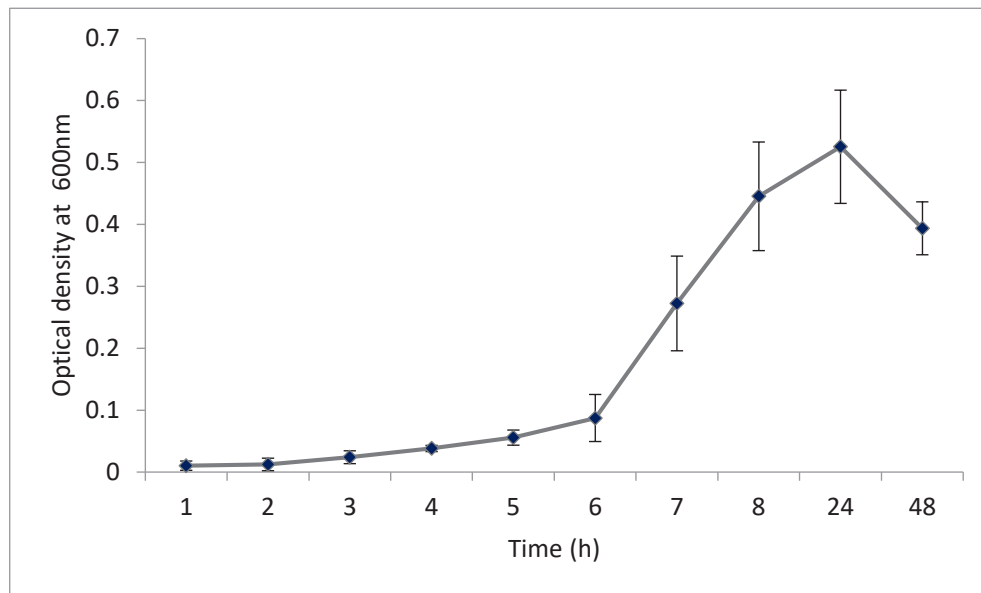


FIGURE 2. Growth curve of *P. vulgaris* in nutrient broth at 37 °C

GROWTH INHIBITORY TEST

The bacterial growth became increasingly inhibited as the concentration of ZnO NPs increased as determined using the turbidity method (Figure 3). The results showed a significant difference ($p < 0.05$) in the growth inhibition of *P. vulgaris* exposed to 50 and 100 $\mu\text{g/mL}$ of ZnO NPs for 24 h compared to the negative control, with

the resultant values of 67.07 ± 4.45 and $76.21 \pm 1.91\%$, respectively. However, there was no significant difference ($p > 0.05$) in growth inhibition reported at 10 $\mu\text{g/mL}$ of ZnO NPs with respect to negative control with the resultant value of $1.66 \pm 0.66\%$ at 24 h, while the positive control showed $91.15 \pm 10.06\%$ growth inhibition. The bacterial colonies grown on LB agar were as shown in Figure 4 and the percentage of growth inhibition of *P.*

vulgaris for colony count method was as presented in Figure 5. Similar to turbidity method, the colony count results reported a significant decrease ($p < 0.05$) in bacterial growth upon exposure to 50 and 100 $\mu\text{g/mL}$ of ZnO NPs for 24 h compared to the negative control, with

the resultant values of 80.94 ± 3.38 and $87.49 \pm 3.29\%$, respectively. However, no significant difference ($p > 0.05$) was reported at 10 $\mu\text{g/mL}$ compared to negative control with the resultant value of $3.61 \pm 1.20\%$ of growth inhibition. The positive control showed $100 \pm 0\%$ growth inhibition.

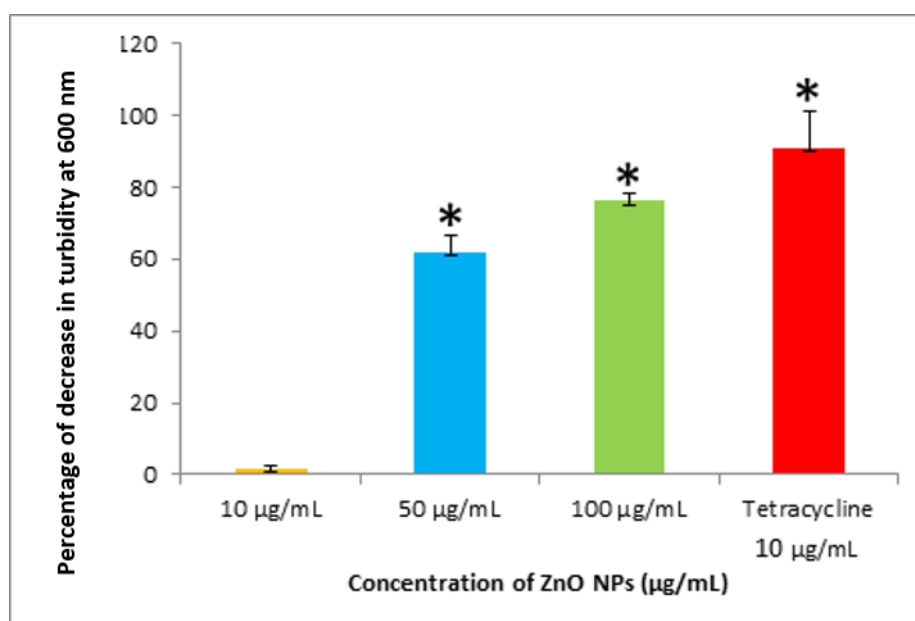


FIGURE 3. Percentage of growth inhibition in *P. vulgaris* upon exposure to ZnO NPs for 24 h in nutrient broth by turbidity method. *indicates $p < 0.05$ between the control and the tested concentrations of ZnO NPs. Tetracycline was used as the positive control

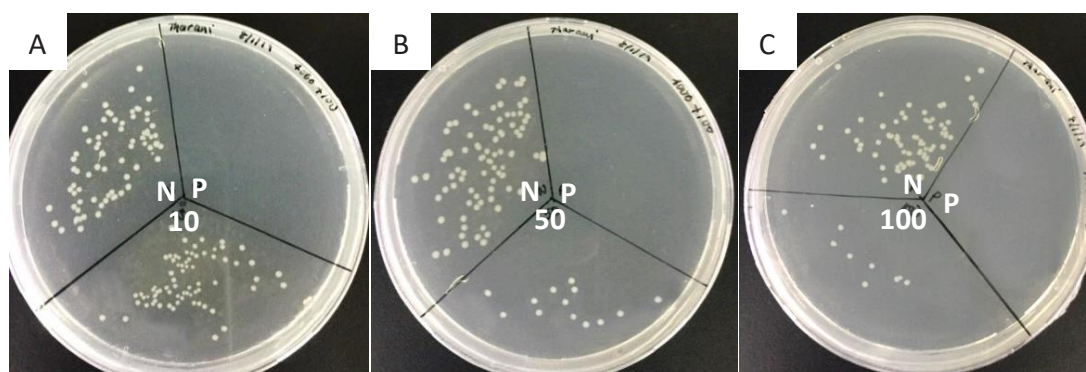


FIGURE 4. Bacterial colonies on LB agar for negative control (N), positive control (P) and bacterial cells exposed to 10 $\mu\text{g/mL}$ (A), 50 $\mu\text{g/mL}$ (B) and 100 $\mu\text{g/mL}$ (C) of ZnO NPs for 24 h

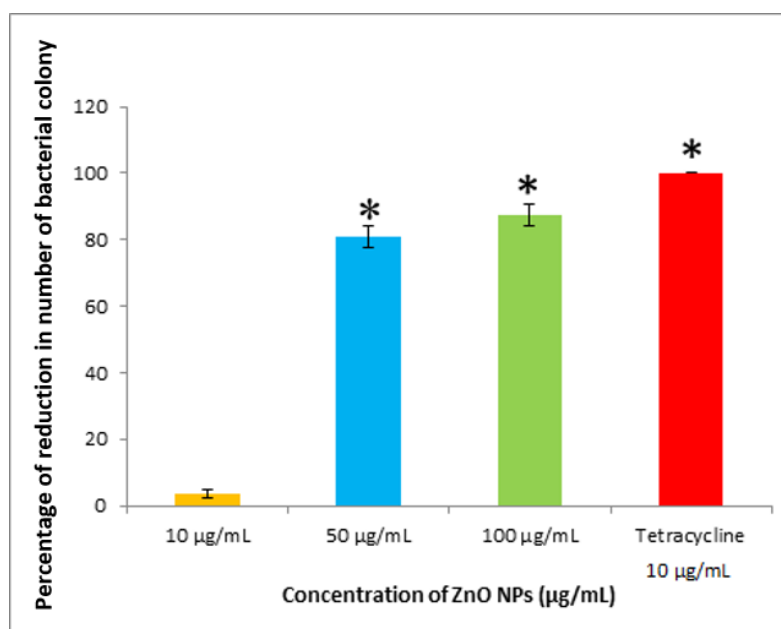


FIGURE 5. Percentage of decrease in number of bacterial colony upon exposure to ZnO NPs for 24 h in LB agar. *indicates $p < 0.05$ between control and tested concentrations of ZnO NPs. Tetracycline was used as the positive control

Similar to the results in the present study, a study by Sirelkhatim et al. (2015) which tested on *Staphylococcus aureus* and *Escherichia coli* showed an increase in antibacterial activity as the concentration of ZnO NPs increased from 6 to 7 mM with reported values of 10.0 and 5.0% viable cells at 6 and 7 mM of ZnO NPs for 8 h. Akbar et al. (2019) investigated the bactericidal effect of ZnO NPs using kill-time analysis and reported that the bacteria *Salmonella typhimurium* and *S. aureus* treated with ZnO NPs (1.3 mM) exhibited a considerable reduction in viable cells from $7.97 \log_{10}$ CFU/mL to $1.825 \log_{10}$ CFU/mL for *S. typhimurium* and $3 \log_{10}$ CFU/mL for *S. aureus* at 4 h. In addition, the study also demonstrated a complete growth inhibition for *S. typhimurium* at 8 h and *S. aureus* at 12 h. Furthermore, the size dependent growth inhibitory effect of ZnO NPs with the particle size ranging from 12 to 88 nm on *S. aureus* was demonstrated by Raghupathi et al. (2011) by turbidity method. Their findings showed that the bacterial growth inhibition was indirectly proportional to the particle size with the smallest size of NPs causing the highest growth inhibition.

Besides, the earlier study showed that the antibacterial properties of NPs were influenced by the size and concentration of NPs (Khezerlou et al. 2018)

and the treatment time with bacteria (Mirzaei & Darroudi 2017). They also proposed three possible mechanisms responsible for the bacterial growth inhibition which were the production of high level of ROS due to the interaction of NPs on bacterial surface, damage to the bacterial cell wall by the accumulation of NPs on bacterial surface (Raghupathi et al. 2011), and liberation of zinc ions into the surrounding medium containing ZnO NPs and causing enzyme disruption and defective protein metabolism (Sirelkhatim et al. 2015).

DETERMINATION OF ROS AND LP

The DCFH-DA assay was used to determine the amount of ROS produced in bacterial cells upon treatment with ZnO NPs for 24 h. The fluorescence of DCF increased as the concentration of ZnO NPs increased. In Figure 6, the results showed a significant ($p < 0.05$) increase in intracellular ROS production for treatment with 50 and 100 µg/mL of ZnO NPs at 24 h compared to the negative control, with the reported values of 388.67 ± 26.07 and $510.90 \pm 108.53\%$, respectively. However, no significant ($p > 0.05$) difference in ROS production was reported at 10 µg/mL of ZnO NPs compared to negative control with the resultant value of $36.90 \pm 6.10\%$. The positive control for bacterial suspension treated with 5% of H_2O_2 showed $1055.48 \pm 133.82\%$ increase in ROS

production. Furthermore, the BODIPY assay was used to demonstrate the lipid peroxidation induced by ZnO NPs in bacterial cells. The percentage of increase in lipid peroxidation on *P. vulgaris* followed a similar trend with ROS production. The results presented in Figure 7 demonstrated that the fluorescent intensity of BODIPY increased as the concentration of ZnO NPs increased

and showed a significant difference ($p < 0.05$) in lipid peroxidation on bacterial cells exposed to 50 and 100 $\mu\text{g/mL}$ of ZnO NPs for 24 h compared to the negative control, with the resultant values of 135.34 ± 21.72 and $328.77 \pm 44.36\%$, respectively. However, there was no significant ($p > 0.05$) difference showed at 10 $\mu\text{g/mL}$ of ZnO NPs compared to negative control with the reported value of $20.69 \pm 7.47\%$. The positive control showed $577.33 \pm 49.22\%$ increase in LP level.

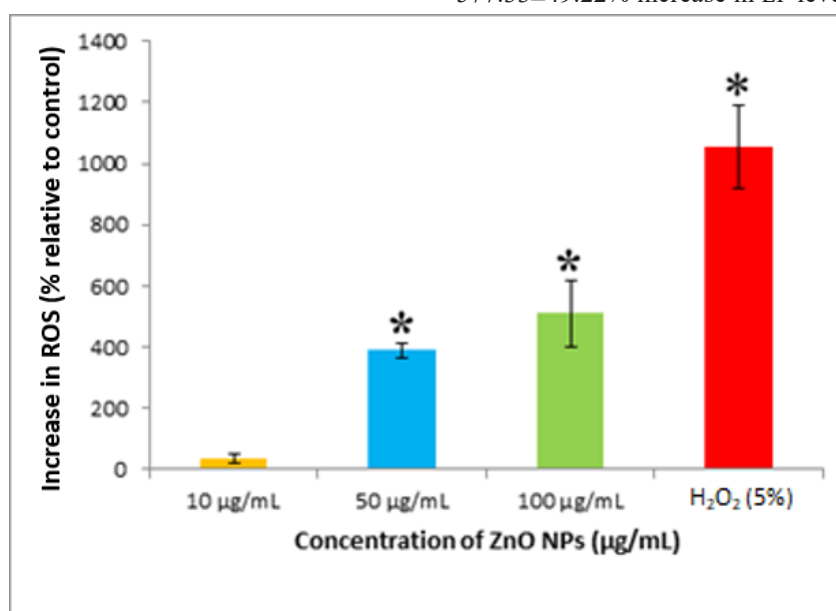


FIGURE 6. Percentage increase in ROS production in *P. vulgaris* upon exposure to ZnO NPs for 24 h in nutrient broth by DCFH-DA assay. *indicates $p < 0.05$ between control and tested concentrations of ZnO NPs, and 5% hydrogen peroxide was used as the positive control

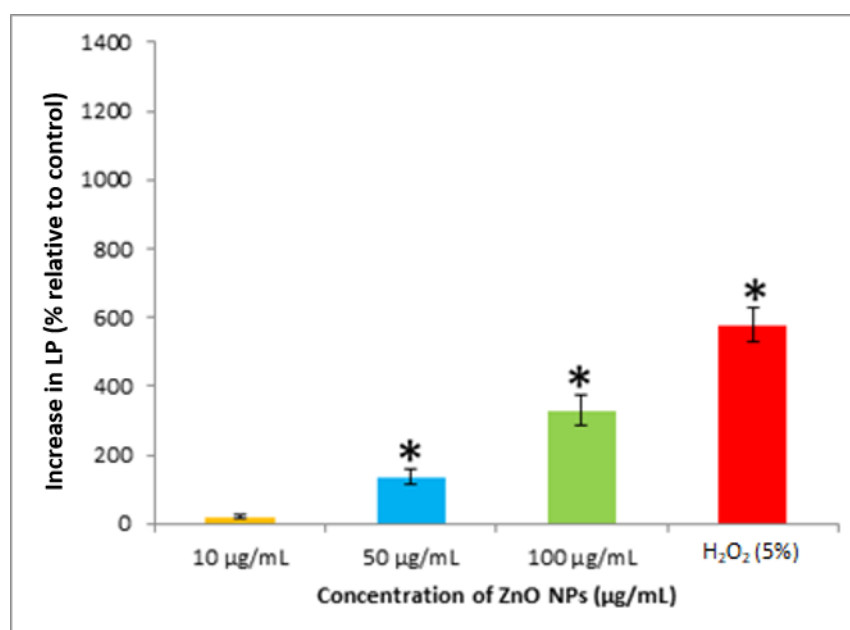


FIGURE 7. Percentage increase in lipid peroxidation in *P. vulgaris* upon exposure to ZnO NPs for 24 h in nutrient broth using BODIPY assay. *indicates $p < 0.05$ between control and tested concentrations of ZnO NPs, and 5% hydrogen peroxide was used as the positive control

It was clearly evident from the results of the present study that the increase in the levels of ROS and LP resulted in the greater bacterial growth inhibition as the concentration of ZnO NPs increased. The interaction of ZnO NPs on bacteria can cause oxidative stress on the bacterial membrane by releasing high amount of ROS and result in killing the bacteria (Gupta et al. 2019). The ROS which include peroxide, hydrogen peroxide, hydroxyl and super oxides are the substances damaging the membrane integrity (Manyasree et al. 2018). Dutta et al. (2012) illustrated the role of ROS and LP in bacterial growth inhibition using bare ZnO NPs (35 mg/100 mL media) and thioglycerol (TG) capped ZnO NPs (55 mg/100 mL broth) against *E. coli* in the presence of histidine which worked as an antioxidant to scavenge ROS to confirm the ROS-mediated antibacterial effect of ZnO NPs. The inhibition of bacterial growth was reduced as the concentration of histidine was increased from 15 mg to 45 mg/100 mL culture medium for both ZnO NPs and TG capped ZnO NP-treated suspensions with the corresponding decrease in ROS formation and malondialdehyde (MDA) equivalents. It was shown from the study that ZnO NPs caused oxidative stress to bacterial cell by inducing excess ROS production which in turn resulted in membrane lipid peroxidation

and growth inhibition. Kumar et al. (2011) reported 21 and 32% increase in ROS production with 25.8 and 49% increase in LP when *E. coli* was treated for 60 min with 8 and 80 $\mu\text{g/mL}$ of ZnO NPs, respectively. Similar results were reported for *Streptococcus pyogenes* when treated with different concentrations of ZnO NPs for 24 h, where dose-dependent ROS and LP production were observed with the corresponding bacterial growth inhibition (Liang et al. 2020).

The lipid peroxidation happens when cells undergo unmanageable stress condition where the hydrogen from the lipid layer is taken away due to initiation of ROS production and then converted to a fatty acid radical ion. This becomes a threat to the permeability of cell and causes loss in membrane integrity, membrane selectivity and fluidity (von Moos & Slaveykova 2014). The critical mechanisms involved in the antibacterial activity of NPs are the membrane protrusion and leakage due to LP and resulting in the leakage of intracellular organelles and eventually cell death (Agarwal et al. 2018).

BINDING OF NPS ON BACTERIAL SURFACE

The functional groups that were responsible for binding ZnO NPs on the bacterial cell surface were identified

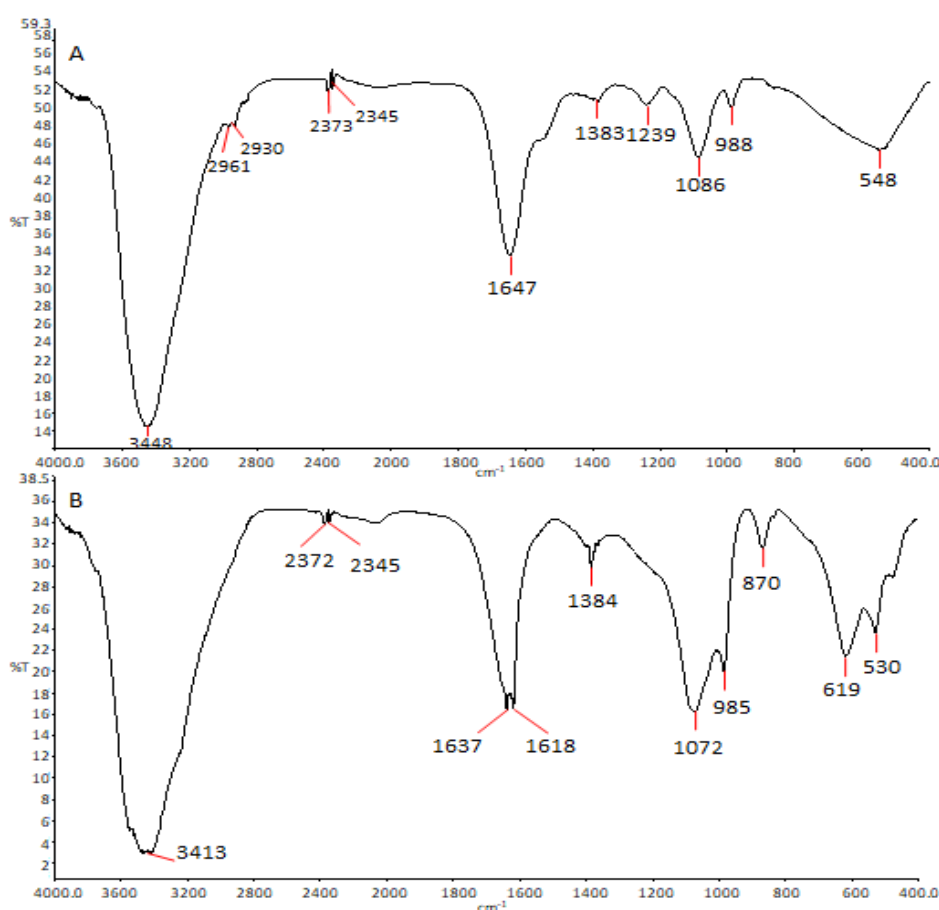


FIGURE 8. The Fourier transform infrared spectroscopy (FTIR) spectrum of *P. vulgaris* (negative control) (A) and *P. vulgaris* with 100 $\mu\text{g/mL}$ ZnO NPs for 24 h (B)

using FTIR as shown in Figure 8. The functional groups were identified from FTIR spectrum by comparing the peaks shifted between the control and the bacterial suspension exposed to 100 µg/mL of ZnO NPs for 24 h. The peak from 2930 to 2961 cm⁻¹ corresponded to alkane with C-H stretching (Silverstein et al. 1981), amine with N-H bending at 1618 cm⁻¹ (University of Colorado 2011a), acid with C-O stretching at 1299 cm⁻¹ (Silverstein et al. 1981), and alkene with =C-H bending at 870 cm⁻¹ (University of Colorado 2011b).

Formation of peak shifts in the treated sample indicated that the structure of the *P. vulgaris* membrane was altered due to the binding of ZnO NPs, hence the new functional groups like amine and alkene were detected in FTIR spectrum. Besides the formation of new peaks in the treated *P. vulgaris*, some functional groups were missing when compared to the control spectrum. The peaks missing at 2930-2961 and 1299 cm⁻¹ were from the alkane and acid group, respectively (Silverstein et al. 1981). The FTIR spectrum for *U. lactuca*-fabricated ZnO NPs showed a broad absorption band at 3418 cm⁻¹ that possibly assigned to H bond in alcohol and the peaks at 1634.00 and 620.93 cm⁻¹ probably due to ZnO stretching and deformation vibration (Iswarya et al. 2018).

CONCLUSIONS

The present study demonstrated the sensitivity of *P. vulgaris* to ZnO NPs treatment and showed a dose-dependent increase in bacterial growth inhibition with increasing concentrations of ZnO NPs. The treatment of ZnO NPs resulted in a significant antibacterial activity on *P. vulgaris* through both bacteriostatic and bactericidal effects. The results also showed the induction of oxidative stress in bacterial cells by ZnO NPs as evident from the dose-dependant increase in ROS and LP. Furthermore, the results also demonstrated the possible involvement of the functional groups such as amine, acid, alkane and alkene groups from the bacterial cell wall in binding ZnO NPs to the bacterial surface. Overall, the present study illustrated the sensitivity of *P. vulgaris* to ZnO NPs treatment.

ACKNOWLEDGEMENTS

This research work was funded by Universiti Tunku Abdul Rahman Research Fund and Ministry of Education, Malaysia (Grant No. FRGS-1-2014-SG03-INTI-02-1).

REFERENCES

- Agarwal, H., Menon, S., Kumar, S.V. & Rajeshkumar, S. 2018. Mechanism study on antibacterial action of zinc oxide nanoparticles synthesized using green route. *Chemico-Biological Interactions* 286: 60-70.
- Akbar, A., Sadiq, M.B., Ali, I., Muhammad, N., Rehman, Z., Khan, M.N., Muhammad, J., Khan, S.A., Rehman, F.U. & Anal, A.K. 2019. Synthesis and antimicrobial activity of zinc oxide nanoparticles against foodborne pathogens *Salmonella typhimurium* and *Staphylococcus aureus*. *Biocatalysis and Agricultural Biotechnology* 17: 36-42.
- Djearamane, S., Wong, L.S., Lim, Y.M. & Lee, P.F. 2020. Oxidative stress effects of zinc oxide nanoparticles on fresh water microalga *Haematococcus pluvialis*. *Ecology, Environment and Conservation* 26(2): 663-668.
- Djearamane, S., Lim, Y.M., Wong, L.S. & Lee, P.F. 2019. Cellular accumulation and cytotoxic effects of zinc oxide nanoparticles in microalga *Haematococcus pluvialis*. *PeerJ* 7: e7582.
- Drummen, G.P., van Liebergen, L.C.M., den Kamp, J.A.F.O. & Post, J.A. 2002. C11-BODIPY (581/591), an oxidation-sensitive fluorescent lipid peroxidation probe: (micro) spectroscopic characterization and validation of methodology. *Free Radical Biology and Medicine* 33(4): 473-490.
- Dutta, R.K., Nenavathu, B.P., Gangishetty, M.K. & Reddy, A.V.R. 2012. Studies on antibacterial activity of ZnO nanoparticles by ROS induced lipid peroxidation. *Colloids and Surfaces B: Biointerfaces* 94: 143-150.
- Elshama, S.S., Abdallah, M.E. & Abdel-Karim, R.I. 2018. Zinc oxide nanoparticles: Therapeutic benefits and toxicological hazards. *The Open Nanomedicine Journal* 5: 16-22.
- Gupta, A., Mumtaz, S., Li, C.H., Hussain, I. & Rotelo, V.M. 2019. Combatting antibiotics-resistant bacteria using nanomaterial. *Chemical Society Reviews* 48(2): 415-427.
- Iswarya, R., Vaseeharan, B., Kalyani, S., Banumathi, B., Govindarajan, M., Alharbi, N.S., Kadaikunnan, S., Al-Anbr, M.N., Khaled, J.M. & Benelli, G. 2018. Facile green synthesis of zinc oxide nanoparticles using *Ulva lactuca* seaweed extract and evaluation of their photocatalytic, antibiofilm and insecticidal activity. *Journal of Photochemistry and Photobiology, B: Biology* 178: 249-258.
- Khezerlou, A., Alizadeh-Sani, M., Azizi-Lalabadi, M. & Ehsani, A. 2018. Nanoparticles and their antimicrobial properties against pathogens including bacteria, fungi, parasites and viruses. *Microbial Pathogenesis* 123: 505-526.
- Kumar, A., Pandey, A.K., Singh, S.S., Shanker, R. & Dhawan, A. 2011. Engineered ZnO and TiO₂ nanoparticles induce oxidative stress and DNA damage leading to reduced viability of *Escherichia coli*. *Free Radical Biology and Medicine* 51(10): 1872-1881.
- Kumar, V.V. & Anthony, S.P. 2016. Antimicrobial studies of metal and metal oxide nanoparticles. In *Surface Chemistry of Nanobiomaterials: Application of Nanobiomaterials* Volume 3, edited by Grumezescu, A.M. Kidlington, Oxford: Elsevier Inc. pp. 265-300.
- Liang, S.X.T., Wong, L.S., Lim, Y.M., Lee, P.F. & Djearamane, S. 2020. Effects of zinc oxide nanoparticles on *Streptococcus pyogenes*. *South African Journal of Chemical Engineering* 34: 63-71.

- Manyasree, D., Kiranmayi, P. & Kolli, V.R. 2018. Characterization and antibacterial activity of ZnO nanoparticles synthesized by co precipitation method. *International Journal of Applied Pharmaceutics* 10(6): 224-228.
- Mirzaei, H. & Darroudi, M. 2017. Zinc oxide nanoparticles: Biological synthesis and biomedical applications. *Ceramics International* 43(1): 907-914.
- Mishra, P.K., Mishra, H., Ekielski, A., Talegaonkar, S. & Vaidya, B. 2017. Zinc oxide nanoparticles: A promising nanomaterial for biomedical applications. *Drug Discovery Today* 22(12): 1825-1834.
- Raghupathi, K.R., Koodali, R.T. & Manna, A.C. 2011. Size-dependent bacterial growth inhibition and mechanism of antibacterial activity of zinc oxide nanoparticles. *Langmuir* 27(7): 4020-4028.
- Ranjbar-Omid, M., Arzanlou, M., Amani, M., Al-Hashem, S.K.S., Mozafari, N.A. & Doghaheh, H.P. 2015. Allicin from garlic inhibits the biofilm formation and urease activity of *Proteus mirabilis* in vitro. *FEMS Microbiology Letters* 362(9): fnv049.
- Reiniers, M.J., van Golen, R.F., Bonnet, S., Broekgaarden, M., van Gulik, T.M., Egmond, M.R. & Heger, M. 2017. Preparation and practical applications of 2',7'-Dichlorofluoresceinin redox assays. *Analytical Chemistry* 87(7): 3853-3857.
- Silverstein, R.M., Bassler, G.C. & Morrill, T.C. 1981. *Spectrometric Identification of Organic Compounds*. 4th ed. New York: John Wiley and Sons.
- Sirelkhatim, A., Mahmud, S., Seeni, A., Kaus, N.H.M., Ann, L.C., Bakhori, S.K.M., Hasan, H. & Mohamad, D. 2015. Review on zinc oxide nanoparticles: Antibacterial activity and toxicity mechanism. *Nano-Micro Letters* 7(3): 219-242.
- University of Colorado. 2011a. IR spectroscopy tutorial: Amines. <https://www.orgchemboulder.com/Spectroscopy/irtutor/aminesir.shtml>. Accessed on 27 April 2021.
- University of Colorado. 2011b. IR spectroscopy tutorial: Alkenes. <https://orgchemboulder.com/Spectroscopy/irtutor/alkenesir.shtml>. Accessed on 27 April 2021.
- Varadavenkatesan, T., Lyubchik, E., Pai, S., Pugazhendhi, A., Vinayagam, R. & Selvaraj, R. 2019. Photocatalytic degradation of Rhodamine B by zinc oxide nanoparticles synthesized using the leaf extract of *Cyanometra ramiflora*. *Journal of Photochemistry and Photobiology B: Biology* 119: 111621.
- von Moos, N. & Slaveykova, V.I. 2014. Oxidative stress induced by inorganic nanoparticles in abteria and aquatic microalgae-state of the art and knowledge gaps. *Nanotoxicology* 8(6): 605-630.

*Corresponding author; email: sinouvassane@utar.edu.my